Progress In Electromagnetics Research, PIER 13, 115–147, 1996

GEOMETRICAL OPTICS OF GUIDED WAVES IN WAVEGUIDES

M. Hashimoto

1. Introduction

Since around 1970, the advent of low-loss optical fibers and their associated technologies added new aspects to the advance of Maxwell's wave optics. Some of them pertained to the mathematical development of the asymptotic theory of Maxwell's equations. In the early days of fiber optics, a lot of people were involved in complicated mathematical problems subject to the medium environment including inhomogeneous anisotropic materials. Design technologies therefore demanded simpler theories that described the principal characteristics of modal waves propagating along multimode fibers [1]. The use of ray optics was very instructive for intending designers, beginners and experts, so that the

ray-optical considerations contributed greatly to the establishment of the design theory of multimode optical fibers. Although the recent technology has shifted to the monomode fiber communications, the need for the establishment of the simplest theory in the monomode fiber system may perhaps remain unchanged. The ray approaches are still useful for understanding the propagation properties of guided light in a wider range of wavelengths. However, certain questions may arise as to the ray tracing in an outer clad region where the ray field is evanescent and thus invisible because of its exponential decay.

For instance, the modal rays are associated with the modal waves and travel in zigzags between two dielectric interfaces. These rays give rise to the interference of two waves coming from upper and lower interfaces. This interference or resonance results in an eigenstate of the modal wave. If, however, the ray of a narrow beam wave is reflected upon the dielectric interface, the ray shift, or the Goos-Hänchen shift, takes place at the reflection point [2]. Nevertheless, no ray shift takes place when the modal rays mentioned above are reflected, as illustrated in standard text books. There are no inconsistencies between these two theories. The former deals with the dynamical rays whereas the latter deals with the stationary rays. These two rays become coincident in continuous isotropic media but different in anisotropic media or isotropic media including discontinuous interfaces. The stationary ray is defined as the locus of wave-normal vectors which are strictly perpendicular to the wavefronts, thus denoting the direction of propagation of the wave. On the other hand, the dynamical ray is defined as the path of a wavepacket. In this Chapter, the dynamical ray and the stationary ray are called the energy ray and the wave-normal ray, respectively. The dynamical theory of geometrical optics is historically established by the ray tracing of energy rays [3]. Despite the most attractive features, however, Hamilton's dynamical approach fails at discontinuous boundaries such as an air-dielectric interface in a dielectric rod. For this reason, the stationary optics has newly been developed and been illustrated by describing the results to be expected in the dynamical optics or in Maxwell's wave optics.

It is the purpose of the present Chapter to give a brief review of the recent development of the stationary optics described in terms of wave-normal rays [4–20], and thus it is not the purpose to give a self-contained paper that provides the full theory the readers can follow. The wave-normal ray description is useful for modal waves in visible

and invisible regions. It is shown that the stationary theory of geometrical optics can be deduced from Maupertuis' variational principle. It is also shown that the conventional ray description, on the other hand, is obtained from Hamilton's variational principle. Comparisons between the two theories are given from a purely physical point of view. The contents to be presented here are partly based on an invited talk at the Seminar on Analytical and Numerical Methods in Electromagnetic Wave Theory, June 3-8, 1991, Adana, Turkey. Because of the limited space, only the main ideas are outlined. The interested reader should refer to the references cited there or the more extended review paper in [21].

2. Historical Note

In dynamics of a wavepacket of light, Professor Synge was primarily concerned with Hamilton's mathematical works collected in *Mathematical Papers of Sir William Rowan Hamilton* [22]. Synge studied Hamilton's variational principle [23] subject to the conservation law of energy $\mathrm{F}(\mathbf{r}, \mathbf{p}, \omega) = 0$ where $\mathbf{r}$ is the position vector, $\mathbf{p}$ is the normalized wavevector ($|\mathbf{p}|$ = refractive index (= n)), and ω is the angular frequency. The variational principle was written in the form slightly different from the well-known form in nonrelativistic quantum mechanics. He then showed that all paths of energy rays are determined from Hamilton's law written in Euler's form in which the independent variables of the Lagrangian function are $\mathbf{r}$ and $\mathbf{p}$. The variation of ω, which results from the independent variations of $\mathbf{r}$ and $\mathbf{p}$ in $\mathrm{F}(\mathbf{r}, \mathbf{p}, \omega) = 0$, produces a sum of wavelets operated by different frequencies, namely, a wavepacket in time domain. Thus, the principle provides the path of the dynamical motion of a wavepacket. The theory is named Hamilton's optical method [24] or simply Hamiltonian optics. If we want further information on the wavefronts of the wave of light, we have to plot equiphase lines, drawing a number of energy rays in the neighborhood of the principal ray. The physical science based on this procedure is called geometrical optics. To distinguish it from others, we use the terminology "the conventional ray optics" or "the conventional geometrical optics".

The ray tracing of wave-normal rays is the technique of determining the wavefronts directly. The curvatures of the wavefronts are traced along the wave-normal ray [6,8,10,11]. When the ray impinges upon a certain discontinuous boundary and penetrates into another medium,

the value of the curvature of the wavefront jumps to a different value. The successive tracing of the wavefronts is found to be equivalent to the tracing of a ray bundle of energy rays in space. In the first decade of the twentieth century, Gullstrand [25] first introduced this idea into classical optics, thereby establishing his theory of human eye [26]. After about twenty years, Hastings [27] applied the same idea independently to the design theory of optical lenses. Quite recently, Gullstrand's approach was restudied by several authors [28,29]. Stavroudis named it the generalized ray tracing [29] to extend the idea of ordinary ray tracing to include the calculation of wavefronts.

These authors, however, seem to have been unaware of the fact that the wave-normal rays which they treated have other properties different from what the energy rays have. This is because they were concerned with isotropic media in which all differences between two definitions to the rays disappear. If the value of ω is fixed to a constant ω_0 in the dispersion equation $\mathrm{H} \equiv \mathrm{F}(\mathbf{r}, \mathbf{p}, \omega_0) = 0$, the variational principle by no means produces a wavepacket. Instead, it describes the motion of a stationary wave operated by a single frequency. The original expression of Maupertuis' principle was given in this style (refer to Subsection 3.3) and later altered in a complete style by Lagrange. In the beginning of the nineteenth century, Hamilton pointed out [23] that Maupertuis' principle of least action had a mathematical drawback when it was applied to the dynamical system of motion of a particle. Since then, the principle of least action seems to have lost its validity in physics. We point out that Maupertuis' principle becomes valid again for the stationary system of wavemotion such as the propagation of a wave of monochromatic light in isotropic/anisotropic inhomogeneous media.

3. Variational Principles

It has been shown that there are two ways of discussing the geometrical configurations of a wave in terms of two different rays. Each gives complete information on the wave mechanism of propagation in time-space domain. Basic rules that constitute different ray configurations in the medium environment are deduced from different variational principles [4,5]. These are outlined in this section.

3.1 Ray Concepts..

Figure l(a) shows a schematic of propagation of a plane wave in a homogeneous anisotropic medium. Since the wavefronts are plane, the directions of wave-normal rays are straightforward as indicated by bold lines with arrows. The energy ray is also a straight line (broken line), but it is directed toward the other direction. Figure l(b) shows the case of propagation of a spherical wave. The direction of the energy ray constructed by a superposition of spherical wavelets remains unchanged. On the other hand, the wave-normal rays curve apparently according to the variations of the wavefronts; thus, the ray directions are uniquely determined if the initial shape of the wavefront at an initial position from which the ray starts is given [6,8,10,11].

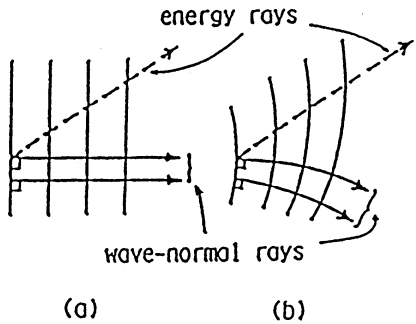

Figure 1. Energy rays (broken lines) and wave-normal rays (bold lines) in an anisotropic medium. The directions of wave-normal rays are defined to be perpendicular to the wavefronts. (From Hashimoto [5], by permission of the IEICE.)

In inhomogeneous and anisotropic media, the ray pictures become more complicated. For example, in magneto-ionic media, the wave-normal pictures may exhibit curious curves that have "cusps" when a spherical wave moves keeping the same radius of curvature of the wavefronts (see Fig. 2). These cuspidal curves of the wave-normal rays contrast well with the gentle curves of the energy rays indicating the paths of energy transport. Obviously, no physical anomalies occur at these cusps. Booker [30] concluded that only the tracing of energy rays is geophysically meaningful.

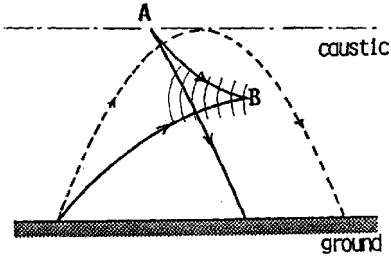

Figure 2. Example of the wave-normal ray (solid line) and the energy ray (broken line) in an inhomogeneous magneto-ionic medium. (After Booker [30].)

3.2 Hamilton's Principle.

Hamilton's dynamical principle provides a systematic plan for writing down the ray equations of dynamical motion of a wavepacket in any system. These ray equations describe the real paths of energy transport. The principle states that the integral of the Lagrangian L over the time axis has a stationary property when the ray moves apart from the real path [23]:

$$\delta \int L dt = 0 \tag{1}$$

The times of departure and arrival, however, are fixed and further the dispersion relation $H = 0$ for waves operated by a central frequency ω_0 is satisfied on the real path (see Fig. 3). The function L is given by

$$L = \mathbf{p} \cdot \mathbf{v_g} - H \tag{2}$$

$$\begin{aligned} H &= H(\mathbf{r}, \mathbf{p}) \\ &= c\ (\mathbf{p}^2/n^2 - 1)/2 \end{aligned} \tag{3}$$

where $\mathbf{v}_g$ is the ray velocity, n is the refractive index specified by a function of the position vector $\mathbf{r}$ and the unit vector $\mathbf{i}_p$ normal to the wavefont, $\mathbf{p}$ is defined by $\mathbf{i}_p$ n, and c is the velocity of light in vacuum.

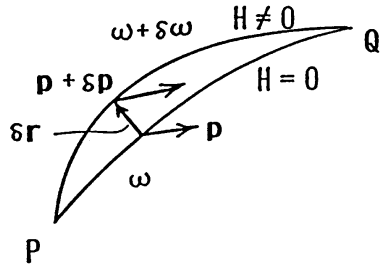

Figure 3. Real path for a stationary wave traveling with $\omega(=\omega_0)$ and p from Point P to Point Q and its virtual path for another stationary wave with $\omega+\delta\omega$ and $\mathbf{p}+\delta\mathbf{p}$. The times of departure at Point P and arrival at Point Q are fixed. These two stationary waves produce a beat wave (dynamical wave) along the energy ray of which the path is independent of the values of $\delta\omega$. (From Hashimoto [21], by permission of the Science House Co., Ltd..)

Letting the first variation of the integral with six degrees of freedom be zero, we obtain the ray equations

$$\frac{d\mathbf{r}}{dt} = \frac{\partial H}{\partial \mathbf{p}} = \frac{c}{n^2}\left(\mathbf{p} - \frac{1}{2}\frac{\partial n^2}{\partial \mathbf{p}}\right) \tag{4}$$

$$\frac{d\mathbf{p}}{dt} = -\frac{\partial H}{\partial \mathbf{r}} = \frac{c}{2n^2}\frac{\partial n^2}{\partial \mathbf{r}} \tag{5}$$

These are basic equations in Hamilton's optics (for example, refer to [21]). The theory of Hamilton's optics is commonly known as a geometrical description in terms of the ray parameters given by (4) and (5). The basic operating principles are comprehensively presented in the book of Maslov and Fedoriuk [31], and the applications to the problem of reflector antennas are in [32].

In what follows, we consider a variation of the functional in a system with three degrees of freedom.

3.3 Maupertuis' Principle and its Modified Form.

The ray equations for the wave-normal rays depicted in space may be obtainable from Maupertuis' original statement "PRINCIPE GÉNÉRAL" reported in 1746 [33, p.36]:

"Lorsqu'il arrive quelque changement dans la Nature, la quantité d'action, nécessaire pour ce changement, est la plus petite qu'il soit possible. La quantité d'action est le produit de la masse des crops, par leur vitesse & par l'espace qu'ils parcourent. Lorsqu'un corps est transporté d'un lieu dans un autre, l'action est d'autant plus grande que la masses est plus grosse, que la vitesse est plus rapide, que l'espace par lequel il est transporté est plus long."

The statement may be expressed in the form

$$\delta S = 0 \tag{6}$$

where

$$S = \int \mathbf{p} \cdot d\mathbf{r} \tag{7}$$

and the integration is carried out over the interval between Points P and Q. The starting point P and the arriving point Q are fixed in space, and instead, the times of departure and arrival are *not* fixed (see Fig. 4). In optics, S is called the optical distance between Points P and Q, which is the distance multiplied by the refractive index.

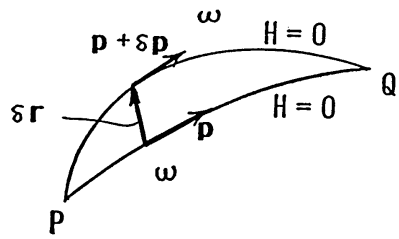

Figure 4. Real path and virtual path for stationary waves traveling with the same value of $\omega(=\omega_0)$ from Point P to Point Q. The times of departure and arrival are not fixed. (From Hashimoto [21], by permission of the Science House Co., Ltd.)

Since the value of ω is assumed to be constant $(= \omega_0)$, the dispersion relation $F = 0$ between **p, r,** and ω is reduced to the dispersion relation $H = 0$ given in an ω-conservative system of motion. The two parameters, **p** and **r**, are thereby restricted by the conservation relation $H = 0$. The vector **p** is now regarded as a function of the vector **r** possessing three arbitrary components, provided that the unit wave-normal vector $\mathbf{i}_p$ is specified in space by $\mathbf{i}_p(\mathbf{r})$. This means that our system of motion has been reduced to a system of three degrees of freedom. Then, taking variations for S with respect to **r**, we obtain [7,21]

$$\frac{d\mathbf{r}}{dt} = \frac{c}{N^2}\mathbf{p}, \qquad \mathbf{p} = \mathbf{i}_p N \tag{8}$$

$$\frac{d\mathbf{p}}{dt} = \frac{c}{N}\frac{\partial N}{\partial \mathbf{r}} \tag{9}$$

where N is the refractive index represented as a function of the single parameter **r**, $\mathrm{N} = \mathrm{N}(\mathbf{r}) \equiv \mathrm{n}(\mathbf{r},\mathbf{i}_p(\mathbf{r}))$. The value of the refractive index written by N should be distinguished from the value of n. The (8) and (9) are the desired expressions for the ray equations of wave-normal rays. Comparisons with Hamilton's ray equations ((4) and (5)) may be helpful in recognizing the difference between the stationary path and the dynamical path.

For two-dimensional cases, we obtain a set of the three equations from (8) and (9)

$$\frac{d\mathbf{r}}{dt} = \frac{c}{n^2}\mathbf{p} \tag{10}$$

$$\frac{d\mathbf{p}}{dt} = \frac{c}{n}\frac{\partial n}{\partial \mathbf{r}} + \frac{1}{R}\frac{c}{n}\frac{\partial n}{\partial \mathbf{i}_p} + \mathbf{i}_p \frac{c}{n^2}\frac{\partial n}{\partial \mathbf{i}_p}\cdot\left(\frac{\partial n}{\partial \mathbf{r}} + \frac{1}{R}\frac{\partial n}{\partial \mathbf{i}_p}\right) \tag{11}$$

$$\frac{dR}{dt} = v_p + R^2\frac{\partial^2 v_p}{\partial s^2} \quad \text{or} \quad \frac{d}{dt}\left(\frac{1}{R}\right) + \frac{v_p}{R^2} = -\frac{\partial^2 v_p}{\partial s^2} \tag{12}$$

where R is the radius of curvature of the wavefront, v_p denotes the phase velocity c/n, and s is the coordinate measured along the wavefront, as shown in Fig. 5. The third equation describes the future events on the wavefront.

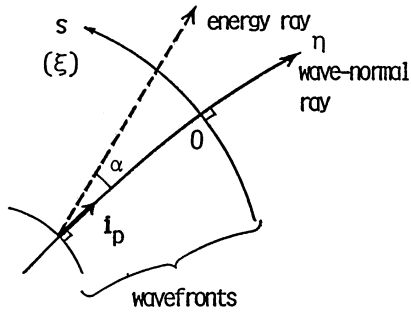

Figure 5. Ray coordinates for a two-dimensional wave. The coordinate η (s = 0) denotes the principal ray.

Equations (10), (11), and (12) are mathematically the same as (8) and (9) in two dimensions. The advantage of using these expressions instead of (8) and (9) is that they present explicit formulas for the radius of curvature of the wavefront, which greatly simplifies the systematic determination of the wavefront. In anisotropic media, these three equations are coupled with each other, and thus, the local nature of wavefronts affects not only the direction of the ray but also the position of the ray [10,11]. Therefore, the ray configurations for the wave-normal rays in anisotropic media depend on the initial shape of the wavefront. If, however, the medium is isotropic (then, the formal expressions for the wave-normal rays and the energy rays become identical), (12) holds independently of the first and second equations, so that any ray path in an isotropic medium is uniquely determined irrespective of whether the shape of the wavefront is planar or spherical. This technique, the ray tracing of wavefronts along an energy ray, is called the dynamic ray tracing in geophysics [34,35], and the generalized ray tracing in optics [29], as described in *Historical Note*.

Another expression for Maupertuis' principle is often given as the principle of least action, containing the two independent parameters **p** and **r** with six degrees of freedom. It is worth noting that this variational expression of six arbitrary parameters leads to another goal, Hamilton's ray equations of dynamical motion, as is well-known in dynamics. The readers should be careful not to confuse this with (6).

Suppose, next, the ray is reflected at the discontinuous interface. The ray field undergoes the phase increment Φ at the reflection point.

If the reflection boundary is the surface of the perfectly conducting material, the value of Φ is exactly equal to π. In most cases, however, the value of Φ decreases as the value of the (complementary) angle of incidence θ_i increases. For the cases when the value of Φ varies with θ_i, the validity of Maupertuis' principle mentioned above is quite unsatisfactory because it does not describe the influence of Φ in the phenomenon of reflection, which is characterized by the high order theory of wave optics. To extend his idea of least action, we subtract Φ/k from the action integral S. The exact value of Φ is unknown for ever unless we solve Maxwell's equations as a boundary value problem. However, since the value of Φ/k is of the order $1/\mathrm{k}$, Φ can be approximated by the phase of Fresnel's reflection coefficient valid for the plane wave incidence upon a plane interface. This modified version of Maupertuis' principle

$$\delta S = 0 \tag{13}$$

with

$$S = \int \mathbf{p} \cdot d\mathbf{r} - \Phi/k \tag{14}$$

will be applied later to the reflection problems encountered frequently in waveguides.

4. Ray Tracing of Wave-Normal Rays and Wavefronts

The ray equations, (8) and (9) or (10), (11) and (12), can be solved efficiently by means of a digital computer, provided that the refractive index of the medium and the specific numerical initial data on the wavefront and the ray position are given [6,8,10]. For a few limited cases [19], we obtain rigorous analytical solutions.

Figure 6a shows an illustrative example [10,11] of the ray tracing for an extraordinary wave in an inhomogeneous anisotropic calcite with

$$v_p = v_0 \sqrt{\frac{1 + g \sin^2 \theta}{1 - by}} \tag{15}$$

where the optic axis and the inhomogeneity axis are assumed to be x and y, respectively, b is constant and θ is the angular coordinate measured in a counterclockwise sense.

The initial wavefront contains convex and concave parts in the upper and lower sides, from which the diverging wavelets and the converging wavelets start upward. The converging ones are focused at the locations which are distributed in space. These distributed focusing points make a line called the caustic that is inaccessible by ray optics. The wavefront tracing as well as the ray tracing will cease on this line (probably placed below the Arabic numerals for S in Fig. 6a).

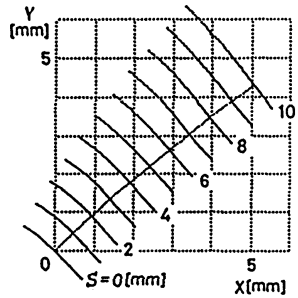

(a) Tracing of a wave-normal ray and associated wavefronts.

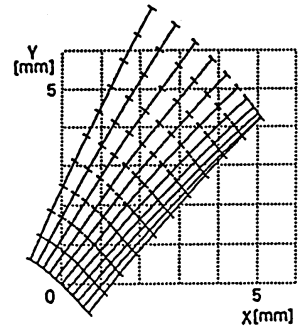

(b) The paths of energy rays and their equiphases calculated by (4) and (5).

Figure 6. Ray tracing in an inhomogeneous anisotropic medium in which the phase velocity is given by (15) with $g = 0.244[mm^{-1}]$, $b = 0.04[mm^{-1}]$ and $v_0/c = 0.603$ [10].

Comparisons are given in Fig. 6b for checking the validity of the method. A number of curved lines represent the energy rays starting with the initial ray directions on the initial wavefront. The cuts marked on the ray curves indicate equiphase planes (wavefronts). Some rays are found to intersect on the lower right corner; these intersects make an optically inaccessible caustic as has already been expected by tracing the wave-normal ray. Results based on the stationary optics (Fig. 6a) and the dynamical optics (Fig. 6b) are in excellent agreement.

5. Tracing of Geometrical Optics Fields along Wave-Normal Rays

The power of light passes through a tube of energy rays, conserving the total energy at any cross section. From this law of energy conservation, we obtain the expression for the intensity I of light along the wave-normal ray [10,21]

$$I = I_0 \frac{R_0}{R} \exp \int_{\eta_0}^{\eta} (\gamma - \tan\alpha \frac{\partial \ln(IR)}{\partial \xi}) d\eta \tag{16}$$

where the subscript 0 denotes the quantities defined at the initial position, α is the angle between the directions of the wave-normal ray and the energy ray (see Fig. 5), ξ is the local coordinate* measured along the wavefront and γ is the known quantity on η. The values of $\tan\alpha$ and γ are given by

$$\tan\alpha = (\partial v_p/\partial\theta)/v_p \tag{17}$$

$$\begin{aligned} \gamma &= \gamma(\xi, \eta) \\ &= \frac{\partial}{\partial \xi} \tan\alpha + \frac{2\tan\alpha}{v_p} \frac{\partial v_p}{\partial \xi} + \frac{R}{v_p} \frac{\partial^2 v_p}{\partial \xi^2} \end{aligned} \tag{18}$$

respectively. The amplitude of the geometrical optics fields can therefore be obtained from (16). Since, in general, the direction of the wave-normal ray differs from that of the energy ray (because $\tan\alpha \neq 0$), the

* Differentiation with respect to s in (12) involved the two types of differential operations with respect to the position $\mathbf{r}$ and the direction $\mathbf{i}_p$. The $\partial/\partial\xi$ indicates the first type of differential operation with respect to $\mathbf{r}$, thus neglecting the variation of $\mathbf{i}_p$ with $\mathbf{r}$. Hence, $\partial/\partial s = \partial/\partial\xi + (1/R)\partial/\partial\theta$. For any homogeneous media, we have $\partial/\partial\xi = 0$.

field amplitude cannot be determined uniquely from the previous data on the wavemotion along the wave-normal ray. The method of field construction thus requires the additional information on the neighboring rays, or exactly speaking, we need to calculate the derivative of the curvature of the wavefronts with respect to ξ (see the second term in the integrand of (16))[10,21]. This term describes a factor of coupling between the two wave-normal rays in anisotropic media. All neighboring rays are thereby coupled so that all initial data on the initial wavefront contribute to the local ray fields. The strength of coupling is weak when the media are weakly anisotropic. This value vanishes absolutely when the media are isotropic. Therefore, the rays are decoupled in isotropic media. A numerical example for calculating the ray fields in an inhomogeneous calcite by the present method is illustrated in Fig. 7 where the field amplitude on the initial wavefront is assumed to be inhomogeneous and have a peak at a certain point. It is shown that a train of the peaks running away from the initial point makes a line close to the expected path of energy transfer.

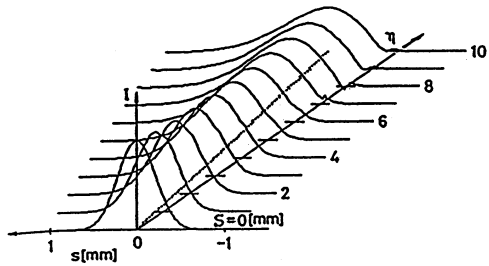

Figure 7. Geometrical optics fields along the wave-normal ray (η axis) calculated in Fig. 6(a). The initial field on the initial wavefront is assumed to be Gaussian. A train of the peaks denoted by a dotted line indicates the path of the maximum intensity of light, which is very close to the energy ray. (Hashimoto and Komiyama [10], by permission of the IEICE.)

6. Total Reflection of Wave-Normal Rays upon a Dielectric Interface

The idea described so far is applied to monochromatic spherical waves emanating from point sources and totally reflected at a dielectric interface. Geometrical rules of total reflection for such waves having curved wavefronts differ from those for a plane wave. The modified version

of Maupertuis' principle provides the law of reflection for stationary waves [12,14]. This will be summarized below.

Figure 8 shows that a two-dimensional spherical wave (a cylindrical wave) starting from Point P is reflected at Point A and propagates toward the observation point Q. Point P' indicates the mirror point of Point P. Point P'' is the real image point of Point P, from which the reflected wave comes directly. The observer looks at Point P'' as an image source instead of the real source although the real propagation undergoes a phase increment Φ by the total reflection. The value of Φ is calculated from Fresnel's reflection formulas, ard thus depends on the value of θ_i. Point P'' is located near Point P' as indicated in Fig. 8 where primes denote differentiation with respect to θ_i and k is the wavenumber in free space. We note that, in general, the (complementary) angle of reflection θ_r is larger than θ_i. However, in the limit of a plane wave incidence where the radius of curvature of the wavefront at the incidence point is infinity, the value of θ_r becomes equal to the value of θ_i. We also note that the phase of the image source must be $\Phi + \Phi''$ when the phase of the original source is zero, and in addition to this, the amplitude of the image source must be equal to the amplitude of the original source, as referred to as the invariant principle [36].

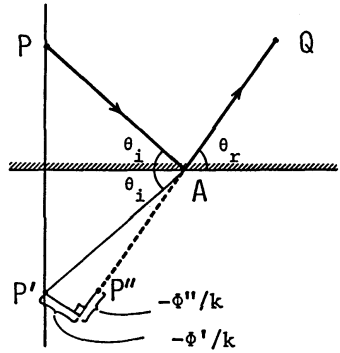

Figure 8. Total reflection of a spherical wave on a plane interface. P is a location of the real source and P″ is its image. $-\Phi''/k$ and $-\Phi/k$ indicates the shifts of the image source from the mirror point P' where primes denote differentiation with respect to θ_i. (From Hashimoto and Zhou [18], by permission of the IEICE.)

The above geometrical rules for the location of the image source can again be stated equivalently as follows:

$$\cos\theta_i - \cos\theta_r = -\frac{\sin\theta_i}{kR_i}\frac{\partial\Phi}{\partial\theta_i} \tag{19}$$

and

$$R_r = R_i + \frac{1}{k}\frac{\partial^2\Phi}{\partial\theta_i^2} \tag{20}$$

where R_i and R_r are the radii of curvature of the incident and reflected wavefronts at Point A, respectively (therefore $\mathrm{R}_i = \overline{PA}$, $\mathrm{R}_r = \overline{P}''A$). Formula (19) is simply derived by applying the variational principle to the "virtual rays" passing near the real path; the real path makes the value of S in (14) minimum as Point A moves on the interface [12,21]. Formula (20) is also derived by applying (19) again to a ray adjacent to the relevant ray, both of which constitute a ray bundle diverging at Point P or Point P″. The (20) is an approximate formula valid for the order of 1/k. The exact expression derived from (19) is [14]

$$\frac{\sin^2\theta_r}{R_r} = \frac{\sin^2\theta_i}{R_i} - \frac{\sin^2\theta_i}{kR_i^2}\left\{\Phi''(\theta_i) + 2\cot\theta_i\Phi'(\theta_i)\right\} \tag{21}$$

Analytical details for these results are given in [12]. The mathematical evidence is exactly involved in the high order asymptotic theory of Maxwell's equations [37]. We do not discuss it any further because we are concerned with the deduction optics deduced from the variational principles and thus the mathematical optics based on Maxwell's equations is beyond the scope.

The dynamical path of a wavepacket starting from Point P and arriving at Point Q should obey Hamilton's rules in the upper (optically denser) medium. However, these rules hold invalid in the lower (optically rarer) medium where the wave of light is evanescent, and therefore, there is no method of tracing the path of an evanescent wavepacket. The dynamical principle has proved to fail at discontinuous boundaries between two media. Nevertheless, the geometrical rules for dynamical waves can be derived from the stationary rules obtained above. To show this, we first note [5] that the path of a wavepacket in time domain coincides with the path of a beam wave which is a "spatial wavepacket" of stationary wavelets in space. The path of the spatial

wavepacket can be determined as follows by complex ray techniques [35,38–42].

Changing the position of the image source P″ downward to the direction Q → A → P″ by the complex amount jb (see Fig. 9), the reflected spherical wave represents, in real space, a Gaussian beam wave propagating along the path AQ. By letting P″ move in complex space, Point P′ (the mirror point of Point P) moves along a line parallel to AQ while Point P moves upside down. Then, the incident energy ray makes an angle θ_r with the interface, and as a result, it crosses the interface at Point A″ shifting to the left from Point A. This shift is called the ray shift or the Goos-Hänchen shift [2].

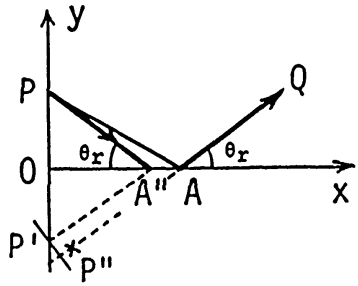

Figure 9. Wave-normal ray, energy ray and ray shift. When the image source P″ shifts to the direction A→P″ in complex space, the reflected spherical wave takes the form of a beam wave whose beam axis coincides with the energy ray. The real source P then shifts upward to the direction A″ →P in complex space, and thus the incident spherical wave also takes the form of a beam wave and this energy ray is directed toward Point A″ making an angle θ_r equal to the angle of reflection. The shift $\overline{A''A}$ is called the ray shift. (From Hashimoto [12], by permission of the IEICE.)

The above simple rule for the location of the image source can be generalized as the *law of image sources* valid in general inhomogeneous media [20,21]. The resulting rules summarized for the particular case in Fig. 8 are applicable to the general cases when the incident ray curves in an inhomogeneous medium and is reflected upon the interface or when the curved incident ray passes through the minimum point at which the ray is reflected and does not impinge on the interface. Then, the *invariant principle of source amplitudes*, as previously mentioned in homogeneous media, must be altered slightly [36,21].

On the other hand, it is also possible to construct the geometrical optics fields by means of Hamilton's optics. The field given as a leading term of an asymptotic solution of the wave equation is described in terms of the ray coordinates α and $\tau(d\tau/dt \equiv c/n^2)$ as follows [31]:

$$\psi(\tau(x,y),\alpha(x,y)) = \psi(0,\alpha(x,y))\sqrt{J(0,\alpha)/J(\tau,\alpha)}\exp -jk\int_0^\tau n^2 d\tau \tag{22}$$

where J is the Jacobian of the transformation from α and τ to x and y,

$$J(\tau,\alpha) = \det \partial(x,y)/\partial(\tau,\alpha) \tag{23}$$

Since the coordinate α is taken to be locally orthogonal to the principal coordinate τ (energy ray), the value of α represents the initial position for the neighboring ray starting at $\tau = 0$. The $J = 0$ corresponds to a singular point of the ray bundle at which the ray field diverges. This point indicates the location of the image source. The reflected wave, a solution in the stationary optics, comes from the image source. We note that the solution obtained in this way in Hamilton's system is *not* identical *but* approximately equal to the stationary solution obtained in Section 5 (refer also to Appendix A); however, both expressions described by the first order of $1/k$ are in complete agreement.

To make it clear, we consider the multiple reflection of a spherical wave of light in a planar waveguide, as shown in Fig. 10. The broken line denotes the path of an energy ray undergoing ray shifts at upper and lower interfaces. The angles of incidence and reflection are the same at every reflection. The solid line is the path of a wave-normal ray traveling in zigzags subject to the stationary law of reflection stated at the beginning of this section. The angle of incidence increases as the ray is *multi*-reflected. Hence, the final angle of reflection at the point of the last reflection, which is equal to the angle of incidence for the broken line (energy ray), becomes much larger than the initial angle of incidence (see Fig. 10).

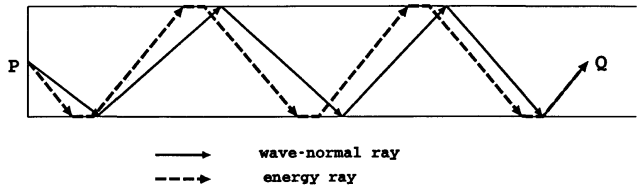

Figure 10. Ray paths in a planar waveguide. The energy ray (broken line) is reflected so that the angles of incidence and reflection are equal. The angle of incidence for the wave-normal ray (solid line) increases as the ray travels to the right.

The difference between these two angles has so far been ignored within the range of order 1/k. However, for the case when the difference is adequately large and thus nonnegligible, the dynamical theory and the stationary theory cannot provide a unique solution. In the limit of $m = \infty$ where m is the number of the multiple reflection, the geometrical optics treatment of order l/k fails absolutely.

7. Applications to Guided Wave Problems

First, we consider whispering gallery waves in a dielectric circular rod in which a progressive wave is incident upon the curved interface from the inside and is reflected backward, and is incident again upon the other part of the interface (see Fig. 11). An infinite number of the wave-normal rays travel along the curved interface. Their envelope appearing in the rod is called the caustic or the distributed source plane from which the rays irradiate the interface.

In familiar text books, the angles of incidence and reflection are shown to be equal, but no answer is given to the question of why the angle of reflection must be equal to the angle of incidence. To give a correct answer, we use the reflection formulas for curved boundaries, instead of (19) and (20) (see the framed equations in Fig. 12) [14].

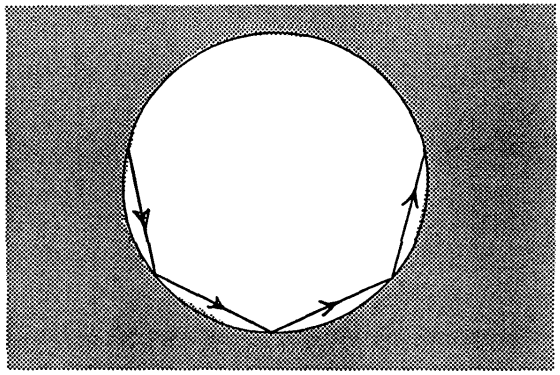

whispering gallery wave in a circular rod

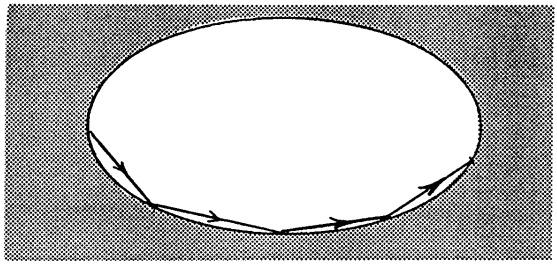

whispering gallery wave in an elliptic rod

Figure 11. Ray configurations of whispering gallery waves. Why is the angle of reflection equal to the angle of incidence upon a circular boundary and why does this not hold upon an elliptic boundary? To explain this, the reflection formulas for the radius of the reflected wavefront (refer to the framed equations in Fig. 12) are applied to the incident spherical waves whose sources are distributed and located on a circular modal caustic [14].

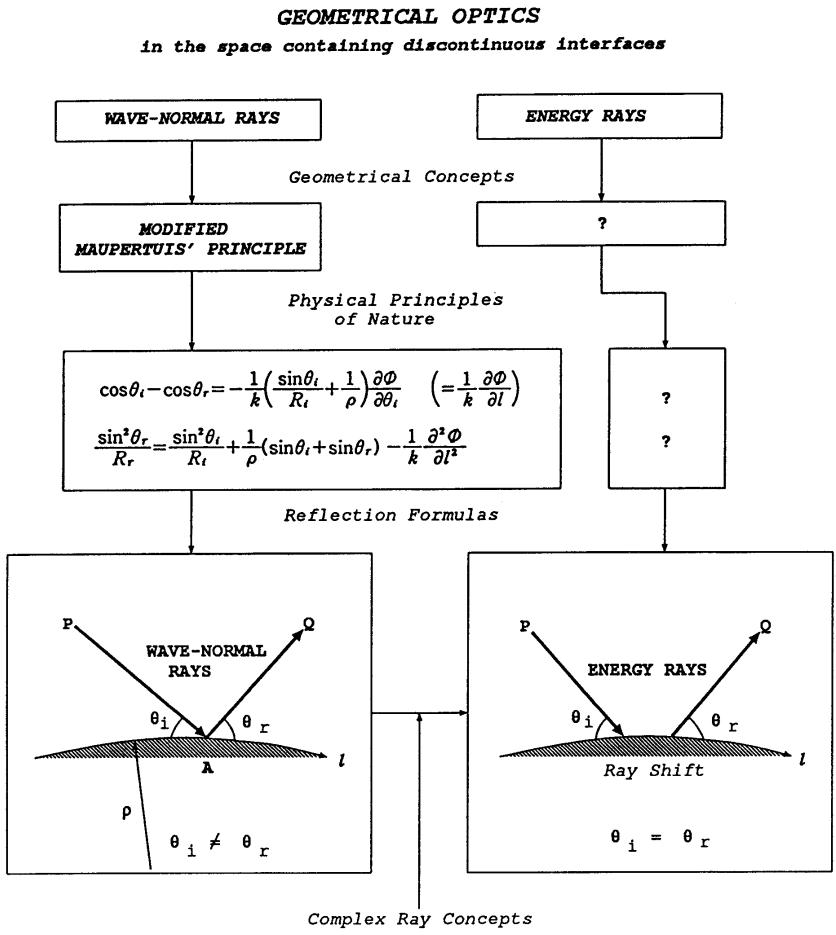

Figure 12. Flow diagram for the stationary theory of deduction optics, illustrating how to explain the phenomena of reflection and ray shift. The dynamical principle describing the geometrical features of energy rays in continuous media becomes invalid for the media containing abrupt discontinuities such as an air-dielectric interface.

The term on the right hand side of (19) should be replaced by $(1/k)(\partial\Phi/\partial l)$ where l is the coordinate along the curved boundary. Let an incident ray come from a certain source point located on the caustic (circle), making an angle θ_i with the reflection boundary. If this boundary is circular, then the neighboring ray starting from the same source point impinges on the boundary, making the same angle θ_i with it at the neighboring point. This means that mathematically $\partial\theta_i/\partial l = 0$ or $\partial\Phi/\partial l = 0$ holds. Therefore, we find $\theta_i = \theta_r$ from $\cos\theta_i - \cos\theta_r = 0$ [21]. The same argument cannot hold in dielectric elliptic rods.

Secondly, we apply the stationary theory to the analysis of dielectric tapered waveguides with the widths of the input end d_1 and the output end d_2, the length L and the refractive index unity. For convenience, the refractive index of the surrounding medium is assumed to be 0.9954. Point P is located on the center of the input end and Point Q is located somewhere on the transverse axis perpendicular to the waveguide axis (the x axis) (see Fig. 13).

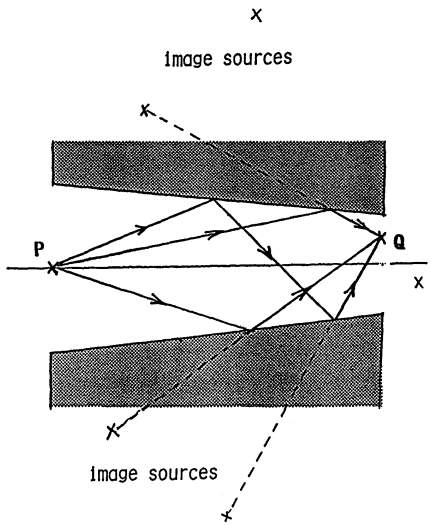

Figure 13. Wave-normal rays in a dielectric tapered waveguide. The real source P is located at the center of the input end. A number of rays arrive at the observation point Q, passing along zigzag paths. Some rays leak out, and as a result, the remaining rays are observed as the guided rays whose sources are located equivalently at the points marked crosses. (From Hashimoto [21], by permission of the Science House Co., Ltd.

There are a number of rays starting from Point P and arriving at Point Q. One is a straight ray and the others are all zigzag rays; they are reflected at the upper and lower interfaces. These zigzag rays come from the image sources directly without receiving any reflection, as have been illustrated in Section 6. Figure 13 shows an example of the locations of the image sources. Such locations shift slightly when Point Q moves along the transverse axis, keeping close to the x axis. However, this shift does not have much effect on calculations of the field distribution unless Point Q moves beyond the range of interest. Therefore, the locations of the image sources are determined by setting Point Q on the x axis. They shift also when Point Q moves along the longitudinal axis (the x axis). The number of the image sources increases as the observer moves toward the right. This effect is nonnegligible.

Geometrical optics fields are calculated as a sum of spherical waves coming from the real source and the image sources, some of which represent totally reflected rays traveling inside the waveguide, undergoing the total reflection at the upper and lower interfaces, and the others represent partially reflected rays or refracted rays. These partially reflected rays scarcely contribute to a description of guided waves, since these describe a leakage of waves leaking out from the waveguide. The leaky ray sources, which are located in real space, can therefore be omitted. The errors caused by this omission are extremely small for the analysis of tapered waveguides, as illustrated in Fig. 14 [15,43].

The evanescent waves generated in the lower (rarer) medium when the total reflection occurs can be characterized by the complex refracted rays whose sources are located in complex space [16,21]. The simplest way to determine the geometrical optics fields for the evanescent waves may be to use the expressions for refracted waves in real space, as omitted above, applying an analytical continuation to it in complex space. The evanescent waves obtained in this way satisfy the boundary conditions at the interfaces. Each wave is an analytically continued solution to the spherical wavelet coming from the source of the real refracted ray. The total evanescent field is given by a sum of the complex refracted fields.

Beam waves can also be obtained by the complex ray techniques; letting Point P shift toward the left by a complex amount $\mathrm{j}kw_0^2$, the spherical wave from Point P in complex space represents in real space a Gaussian beam wave with $1/\sqrt{e}$-waistsize w_0 [39–42]. The image

sources also shift toward the left by the same amount. The resulting complex rays are collected to describe the geometrical optics field of the guided wave excited by the Gaussian beam wave.

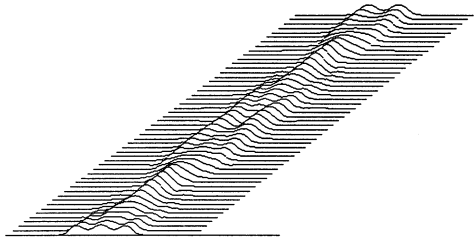

(a) Geometrical optics solution.

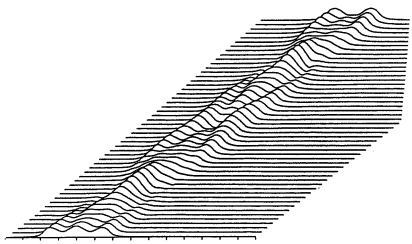

(b) Wave optics solution (BPM solution).

Figure 14. Waves along a dielectric taper [43]. $x = 500\mu$**m-** 1500μ**m.**

Figure 14a shows a numerical example of beam wave propagation for $w_0 = 2.3\,\mu\,m$ [43]. The wavenumber is assumed to be $10\ \mu\,m^{-1}$, the values of d_1 and d_2 are, respectively, $20\,\mu\,m$ and $10\,\mu\,m$, and the value of L is $3000\,\mu\,m$. The waveguide supports several modes along the x axis, so that some high order modes radiate from the interfaces between the input and output ends and a few low order modes remain at the final goal.

The result has been checked by comparing with the beam propagating method (BPM) solution (see Fig. 14b). The BPM solution is a solution of the partial differential equation of parabolic type, as given in the paraxial wave optics deduced from a proper approximation of Maxwell's equations [44]. Although both are in excellent agreement, such a comparison has no significance in testing the validity of the

method because of their different bases of approximation. Analytical comparisons with the wave solution [45] obtained from the geometrical optics solution by means of analytical continuation in a spectral domain may be more fruitful.

8. Summary

The theory of stationary optics for guided waves in waveguides has briefly been reviewed and various rules derived for the stationary ray, called the wave-normal ray, are discussed in comparison with the conventional dynamical optics rules. It has been mentioned that these two definitions are compatible in representing high frequency waves. The ray of light in the stationary optics indicates the direction of motion of stationary waves, which is perpendicular to the wavefronts, and in general, it does not indicate the direction of the transport of energy of waves. We have made a clear distinction between the two descriptions of geometrical optics according to which we have treated a monochromatic wave or a wavepacket.

Figure 15 shows a schematic for the two ways of describing deduction optics. These two theories can be consistent within the range of order 1/k, thus providing the same solution unless we compare their high order terms.

The prominent advantage of the stationary optics is that the ray traveling near the discontinuous interface can always be traced in the visible region if the phase increment due to the reflection is specified by a function of the angle of incidence; we need not calculate the complex ray path to evaluate the effects of the evanescent field in the invisible region. This is summarized in Fig. 12.

The framed question marks denote unknown formulas which can never be derived from Hamilton's dynamical principle. The directions of arrows represent the directions of deduction where R_i or R_r is the radius of curvature of the wavefront of the incident or reflected wave at Point A. The new dynamical theory of optics has been established by letting the source location in the stationary optics shift toward the complex location, and thereby, the well known principle of equal angles for the incident and reflected dynamical waves has been explained.

It is believed that the stationary theory can describe more complicated configurations of motion of three-dimensional waves, the wavefronts of which rotate around the principal ray.

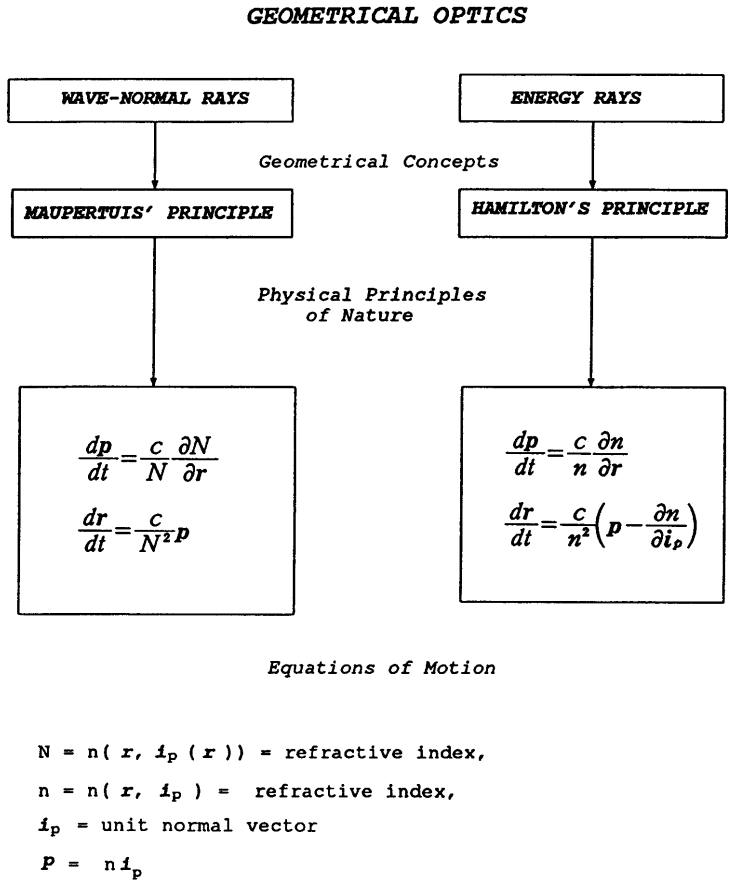

Figure 15. The two theories of deduetion optics in continuous anisotropic media. The stationary theory is deduced from Maupertuis' principle whereas the dynamical theory is deduced from Hamilton's principle.

Acknowledgments

This work was motivated by a talk with Prof. I. Kimura, Kyoto University about the ray tracing of radio waves in ionosphere. The author also expresses his gratitude to Prof. H. Ogura, Kyoto University, who pointed out Prof. Synge's book describing Hamilton's mathematical theory with logical rigor.

Appendix A

A similar idea can also be applied to the problem of refraction. We here outline the law of refraction in comparison with the law of reflection, both of which are deduced from Maupertuis' principle. The exact expressions for the law of reflection, (19) and (21), will again be derived for comparison purposes.

Since the action S in (14) describes an optical distance from the source point P to the observation point Q, we have $S = \overline{PA} + \overline{QA} - \Phi/k$ when point Q is in the upper medium (air) and $S = \overline{PA} + n\overline{QA} - \Psi/k$ when point Q is in the lower medium with refractive index n (see Fig. A1), where Ψ denotes the phase increment due to refraction at the point of incidence (Point A) located on the discontinuous interface.

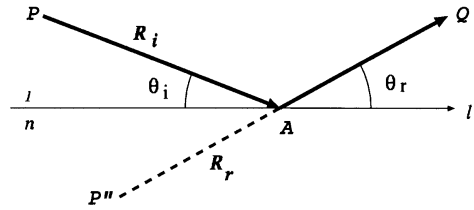

Figure A1a. Reflection of wave-normal rays at a plane interface. The refractive indices of the upper and lower media are unity and n, respectively: $R_i \equiv \overline{PA}$, $R_r \equiv \overline{P}''A$.

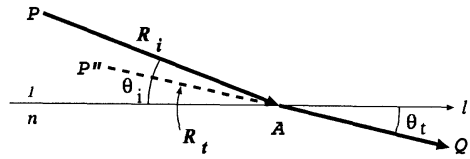

Figure A1b. Refraction of wave-normal rays at a plane interface. The refractive indices of the upper and lower media are unity and n, respectively: $R_i \equiv \overline{PA}$,$R_t \equiv \overline{P}''A$.

Location of Point A is indicated by the coordinate l measured along the interface. Then S is given by a function of l. To minimize the value of S, we differentiate S with respect to l and put $\partial S/\partial l = 0$. From this stationary condition, the laws of reflection and refraction

follow immediately. The resulting formulas for the angles of incidence, reflection and refraction, $\theta_i, \theta_r, \theta_t$, and the radii of curvature of the wavefronts of incident, reflected and refracted waves at point A, R_i, R_r, R_t, are listed below.

$$\cos\theta_r = \cos\theta_i + \frac{\sin\theta_i}{kR_i}\Phi'(\theta_i) \tag{A1}$$

$$n\cos\theta_t = \cos\theta_i + \frac{\sin\theta_i}{kR_i}\Psi'(\theta_i) \tag{A2}$$

$$\frac{\sin^2\theta_r}{R_r} = \frac{\sin^2\theta_i}{R_i} - \frac{\sin^2\theta_i}{kR_i{}^2}\left\{\Phi''(\theta_i) + 2\cot\theta_i\Phi'(\theta_i)\right\} \tag{A3}$$

$$\frac{n\sin^2\theta_t}{R_t} = \frac{\sin^2\theta_i}{R_i} - \frac{\sin^2\theta_i}{kR_i{}^2}\left\{\Psi''(\theta_i) + 2\cot\theta_i\Psi'(\theta_i)\right\} \tag{A4}$$

where primes denote differentiation with respect to θ_i. The first and second equations represent $\partial S/\partial l = 0$, and the last terms on their right hand sides arise from the derivatives of Φ and Ψ with respect to l. Equations (A3) and (A4), respectively, are obtained by differentiating (A1) and (A2) again with respect to l and applying $\partial/\partial l = -(\sin\theta_i/R_i)\partial/\partial\theta_i = -(\sin\theta_r/R_r)\partial/\partial\theta_r = -(\sin\theta_t/R_t)\partial/\partial\theta_t$.

Now suppose that an incident cylindrical wave emanates from Point P and is reflected or refracted at Point A where the values of θ_i and R_i are specified. The wave-normal rays of the reflected or refracted waves are seen to issue directly from the image source P″. The angle θ_r or θ_t and the radius R_r or R_t are determined by (A1)–(A4). This means that locations of Point P″, which we demand to know in constituting the ray solution, are determined exactly.

The geometrical optics fields corresponding to incidence, reflection, and refraction are given by $\psi^i = K_i\exp(-jkr)/\sqrt{r}$, $\psi^r = K_r\exp(-jkr)/\sqrt{r}, \psi^t = K_t\exp(-jknr)/\sqrt{r}$, respectively, where r denotes the distance between Point P″ and Point Q, and Ks are coefficients. The continuity of fields at Point A, $\psi^i + \psi^r = \psi^t$, with reflection coefficient $\Gamma(=\psi^r/\psi^i)$ and transmission coefficient T $(=\psi^t/\psi^i)$, requires

$$K_r = K_i\sqrt{\frac{R_r}{R_i}}\,\Gamma e^{-jk(R_i-R_r)} \tag{A5}$$

$$K_t = K_i \sqrt{\frac{R_t}{R_i}}\, T e^{-jk(R_i - nR_t)} \tag{A6}$$

In the case of total reflection when the lower medium is optically rarer and further the value of θ_i is taken to be less than the critical angle $\theta_c = \cos^{-1} n$, the law of conservation of energy flux holds in the incident ray tube and the reflected ray tube. Although it is evident from $\partial\theta_r/\partial\theta_i \neq 1$ that the cone angles of ray tubes for the wave-normal rays at Point P and Point P$''$ are different, those for the energy rays are identical [36]. This implies that the amplitudes of the real source at Point P and the image source at Point P$''$ are the same; $|K_r| = |K_i|$. Thus, [36]

$$\Gamma = \sqrt{\frac{R_i}{R_r}} e^{j\Phi} \tag{A7}$$

Based on the rule of analytic continuation in mathematics, this mathematical expression is expected to be valid for both real and imaginary values of Φ. Thus, the formula (A7) is extended to both partial and total reflections.

The fields ψ^r and ψ^t obtained above are described in terms of Φ and Ψ. The value of Ψ can however be determined as follows by substituting (A7) into T(=1+ Γ),

$$T = 2\sqrt[4]{\frac{R_i}{R_r}} \cos\left(\frac{\Phi}{2}\right) e^{j\Psi} + 0\left(\frac{1}{k^2}\right) \tag{A8}$$

$$\Psi = \frac{\Phi}{2} - \frac{\Phi''}{4kR_i} \tan\left(\frac{\Phi}{2}\right) + 0\left(\frac{1}{k^2}\right) \tag{A9}$$

The value of Φ remains unknown. The first approximation for Φ may be to use the phase of Fresnel's reflection coefficient, $\Phi_F(\theta_i)$,

$$\Phi_F(\theta) \equiv 2\tan^{-1}\left(\frac{\sqrt{\cos^2\theta - n^2}}{\sin\theta}\right) \tag{A10}$$

which holds valid only for plane wave incidence. The results obtained by this approximation are discussed in the paper "Ray technique for stationary waves in guided wave structures" presented at Mathematical Methods in Electromagnetic Theory (MMET *94), Kharkov, Ukraine, 138–147, Sept. 7–10, 1994.

References

1. For example, see Gloge, D., ed., *Optical Fiber Technology,* IEEE Press, New York, 1976.
2. Kogelnik, H., "Theory of dielectric waveguides," Chap. 2 in *Integrated Optics,* Springer-Verlag, New York, 1975.
3. Arnaud, J. A., *Beam and Fiber Optics,* Academic Press, New York, 1976.
4. Hashimoto, M., "A new aspect of guided wave optics—the basic law of action for modal-ray optics," *Proc. Sino-Japanese Joint Meeting on Optical Fiber Science and Electromagnetic Theory,* Nanjing, China, 87–92, May 12–14, 1987.
5. Hashimoto, M., "Principles for modal waves in guided wave optics," *Trans. IEICE,* Vol. J70-C, No. 11,1455–1465, 1987.
6. Hashimoto, M., and A. Komiyama, "Ray tracing of wave-normal rays," *Trans. IEICE,* Vol. J70-C, No. 10, 1444–1446, 1987; erratum, Vol. J71-C, No. 1, 163, 1988.
7. Hashimoto, M., "On a direct derivation of ray equations from Maupertuis' variational principle," *Trans. IEICE,* Vol. J71-C, No. 2, 324–326, 1988.
8. Komiyama, A., and M. Hashimoto, "Ray tracing of wave-normal rays in an inhomogeneous anisotropic medium," *Trans. IEICE,* Vol. J71-C, No. 2, 327–329, 1988.
9. Hashimoto, M., "The geometrical optics field of guided waves –A geometrical interpretation for the field amplitude–," *Trans. IEICE,* Vol. J71-C, No. 6, 953–956, 1988.
10. Hashimoto, M., A. and Komiyama, "Two-dimensional ray tracing for wavefronts, wave-normal rays and geometrical optics fields," Trans. *IEICE* , Vol. J71-C, No. 7, 980–985, 1988.
11. Hashimoto, M., and A. Komiyama, "New ray tracing for waves in inhomogeneous anisotropic media," *Proc. Int. Symp. Radio Propagat.,* Beijing, China, 93–96, April 18–21, 1988.
12. Hashimoto, M., "The law of total reflection in geometrical optics based on wave-normal rays," *Trans. IEICE.,* Vol. J72-C-I, No. 3, 132 –138, 1989.
13. Hashimoto, M., "Geometrical description for wave-normal rays in an optical waveguide–Geometrical optics for stationary waves," *Proc. Int. URSI Symp.,* Stockholm, Sweden, 303–305, August 14–17, 1989.

14. Hashimoto, M., "The geometrical law of total reflection for wave-normal rays on curved boundaries," *Trans. IEICE,* Vol. J72-C-I, No. 9, 562–564, 1989.
15. Hashimoto, M., and X. J. Zhou, "Geometrical optics analysis for the beam wave propagation in dielectric waveguides," *Proc. Japan-China Joint Meeting on Optical Fiber Science and Electromagnetic Theory,* Fukuoka, Japan, 1–10, October 12–14, 1990.
16. Hashimoto, M., "The geometrical optics of wave-normal rays for totally reflected electromagnetic waves," Trans. $IEICE$, Vol. J73 -C-I, No. 11, 738–740, 1990.
17. Hashimoto, M., "On the wave-normal rays and the reflection coefficients," *Trans. IEICE,* Vol. J74-C-I, No. 3, 97–99, 1991.
18. Hashimoto, M., and X. J. Zhou, "Geometrical optics analysis for the beam wave propagation in dielectric tapered waveguides," *Trans. IEICE,* Vol. E74, No. 9, 2938–2940, 1991.
19. Hashimoto, M., "Spotsizes of the beam waves propagating along a two-dimensional inhomogeneous medium," *Trans. IEICE,* Vol. J75-C-I, No. 1, 1–7, 1992.
20. Hashimoto, M., "The geometrical law of total reflection for wave-normal rays on the discontinuous interfaces in inhomogeneous media," *Trans. IEICE,* Vol. J75-C-I, No. 4, 173–178, 1992; Supplement to a paper on "The geometrical law of total reflection for wave-normal rays on the discontinuous interfaces in inhomogeneous media," *Trans. IEICE,* Vol. J75-C- I, No. 4, 197–199, 1992.
21. Hashimoto, M., "Geometrical optics of guided waves: Stationary optics for modal waves," Chapter One of the book *Analytical and Numerical Methods in Electromagnetic Wave Theory,* edited by Hashimoto, M., Idemen, M., and O. A. Tretyakov, Science House Co. Ltd., Tokyo, 1993.
22. Hamilton, W. R., *The Mathematical Papers of Sir William Rowan Hamilton,* Vol. 1, Cambridge Univ. Press, Cambridge, 1931.
23. Hamilton, W. R., *The Mathematical Papers of Sir William Rowan Hamilton,* Vol. 2, Cambridge Univ. Press, Cambridge, 1940.
24. Synge, J. L., *Geometrical Mechanics and deBroglie Waves,* Cambridge Univ. Press, Cambridge, 1954.
25. Gullstrand, A., "Die reelle optische Abbildung," *Kungl. Svenska Vetenska. Handl.,* Vol. 41, No. 3, 1–119, 1906.
26. Gullstrand, A., "Das allgemeine optische Abbildungssystem," *Kungl. Svenska Vetenska. Handl.,* Vol. 55, 1–139, 1915.

27. Hastings, C. S., "New Methods in Geometrical Optics," Macmillan Company, New York, 1927.
28. Kneisly II, J. A., "Local curvatures of wavefronts in an optical system," *J. Opt. Soc. Am.,* Vol. 54, No. 2, 229–235, 1964.
29. Stavroudis, O. N., *The Optics of Rays, Wavefronts, and Caustics,* Ch. 9, Academic Press, New York, 1972.
30. Booker, H. G., "Propagation of wave-packets incident obliquely upon a stratified doubly refracting ionosphere," *Phil. Trans. Roy. Soc. London,* Vol. A237, 411–451, 1938.
31. Maslov, V. P., and M. V. Fedoriuk, *Semi-Classical Approximation in Quantum Mechanics,* D. Reidel Pub. Co., London, 1981.
32. Hongo, K., Y. Ji, and E. Nakajima, "High-frequency expression for the field in the caustic region of a reflector using Maslov's method," *Radio Sci.,* Vol. 21, No. 6, 911–919, 1986.
33. Maupertuis, P. L. M., "Euvres," Vol. 4, 1965, "Accord de differentes lois de la nature," 3–28, 1744; "Recherche des lois du mouvement," 31–42, 1746.
34. Červený, V., and F. Horn, "The ray series method and dynamic ray tracing system for three-dimensional inhomogeneous media," *Bull. Seism. Soc. Am.,* Vol. 70, No. 1, 47–77, 1980.
35. Červený, V., M. M. Popov, and I. Pšenčlk, "Computation of wave fields in inhomogeneous media—Gaussian beam approach," *Geophys. J. R. Astr. Soc.,* Vol. 70, 109–128, 1982.
36. Hashimoto, M., "On the magnitude of the image source of a spherical and nonspherical wave reflected upon an interface," *Trans. IEICE,* Vol. J75-C-I, No. 8, 561–563, 1992.
37. Brekhovskikh, L. M., *Waves in Layered Media,* Ch. 4, Academic Press, New York, 1960.
38. Keller, J. B., and W. Streifer, "Complex rays with an application to Gaussian beams," *J. Opt. Soc. Am.,* Vol. 61, No. 1, 40–43, 1971.
39. Deschamps, G. A., "Gaussian beam as a bundle of complex rays," *Electron. Lett.,* Vol. 7, No. 23, 684–685, 1971.
40. Felsen, L. B., and S. Y. Shin, "Rays, beams and modes pertaining to the excitation of dielectric waveguides," *IEEE Trans. Microwave Theory Tech.,* Vol. MTT-23, No. 1, 150–161, 1975.
41. Suedan, G. A., and E. V. Jull, "Two-dimensional beam diffraction by a half-plane and wide slit," *IEEE Trans. Antennas Propagat.,* Vol. AP-35, No. 9, 1077–1083, 1987.

42. Hashimoto, M., "Beam waves with sources at complex location," *Electron. Lett.,* Vol. 21, No. 23, 1096–1097, 1985.
43. Hashimoto, H., and M. Hashimoto, "Geometrical optics based on wavenormal rays—Contributions of leaky ray sources to guided waves in dielectric waveguides–," *Proc. Sino-Japanese Joint Meeting on Optical Fiber Science and Electromagnetic Theory,* Xi'an, China, 345-350 October 7–10, 1993; see also, Hashimoto, M., and Hashimoto, H., "Ray-optical techniques in dielectric waveguides," *IEICE Trans. Electron.*, Vol. E77-C, No. 4, 639–646, April 1994.
44. Baets, R., and P. E. Lagasse, "Calculation of radiation loss in integrated-optic tapers and Y-junction," *Appl. Opt.,* Vol. 21, No. 11, 1972–1978, 1982.
45. Cada, M., F. Xiang, and L. B. Felsen, "Intrinsic modes in tapered optical waveguides," *IEEE J. Quantum. Electron.,* Vol. 24, No. 5, 758–765, 1988.